

**The North Dakota Tornadic Supercells of 18 July 2004:  
Issues Concerning High LCL Heights and Evapotranspiration**

David J. Kellenbenz and Thomas J. Grafenauer

NOAA/National Weather Service, Weather Forecast Office, Eastern North Dakota

Jonathan M. Davies

Private Meteorologist

Wichita, Kansas

Accepted to *Weather and Forecasting* – Manuscript No. 2006109

12 April 2007

*Corresponding author:* David J. Kellenbenz, 4797 Technology Circle, Grand Forks, ND 58203

[David.Kellenbenz@noaa.gov](mailto:David.Kellenbenz@noaa.gov)

Phone number: 701-795-5198 Fax number: 701-772-0751

## **Abstract**

On the evening of 18 July 2004, several tornadoes occurred with two supercell thunderstorms over eastern North Dakota. The second and smaller in diameter of these storms produced an F4 tornado in an environment with lifting condensation levels (LCL heights) that were atypically high according to recent statistical studies about supercell tornado environments. Surface dewpoints were also under-forecast by computer models. These two issues are examined in this paper, which provides an overview of this event. The synoptic setting and environment characteristics suggest that evapotranspiration (ET) was responsible in part for enhancing surface moisture. ET likely affected instability and convection initiation. This study also found that the presence of steep low-level lapse rates juxtaposed with low-level convective available potential energy (CAPE) along a surface trough may have contributed to tornado development in a high LCL environment where wind and instability characteristics were otherwise favorable for supporting supercell tornadoes.

## **1. Introduction**

Supercell thunderstorms over eastern North Dakota produced several tornadoes on the evening of 18 July 2004. The smaller of two tornadic supercell storms during this event produced an F4 tornado (Fig. 1). This was only the third F4 tornado documented in North Dakota during the 26 year period from 1979 to 2004 by the National Oceanic and Atmospheric Administration (NOAA) publication *Storm Data*. The environment exhibited large convective available potential energy (CAPE), and significant low-level and deep-layer vertical shear, as seen in many strong and violent tornado events (e.g., Davies and Johns 1993; Rasmussen and Blanchard 1998; Thompson et al. 2003). However, lifting condensation level (LCL) heights and cloud bases were relatively high in the area where the violent tornadic storm developed, as depicted in the 0000 UTC 19 July 2004 mesoanalysis (Fig. 2) from the Storm Prediction Center (SPC; Bothwell et al. 2002). These latter characteristics and associated surface dewpoint depressions did not appear to be strongly supportive of strong or violent tornado development based on recent statistical studies of supercell tornado environments (e.g., Rasmussen and Blanchard 1998; Markowski et al. 2002; Thompson et al. 2003). Another interesting aspect of this case was the under-forecast of surface moisture by operational forecast models. This may have reflected, in part, the inability of the models to properly account for evapotranspiration (ET) (Holt et al. 2006). These observations

motivated a study of the synoptic and mesoscale environment associated with this event, which is presented in this paper.

The following section is a brief documentation of the tornadoes that occurred on 18 July 2004. An analysis of the associated synoptic and mesoscale environment over eastern North Dakota, including common parameters used in supercell tornado forecasting, will then be presented. The possible effects of ET on boundary layer moisture, CAPE, and convection initiation will be considered. The low-level thermodynamic characteristics potentially relevant to tornado development in a relatively high LCL environment will also be reviewed. A discussion and summary will conclude the paper.

## **2. Overview of event**

There were at least eight distinct tornado reports in the Grand Forks Weather Forecast Office (WFO) County Warning Area (CWA) during the evening of 18 July 2004. The damage paths and initiation times of these tornadoes, based on two damage survey teams from the Grand Forks WFO, are shown in Fig. 3a. The initial supercell storm developed after 2300 UTC near Grand Forks, and moved south. Several sequential mesocyclones, identified on radar, developed on the southwestern side of this storm between 0000 UTC and 0300 UTC (19 July 2004). These mesocyclones produced tornadoes, two of which were rated F2 on the Fujita scale and caused around \$750,000 in damage. The strongest tornado, rated F4, occurred with a separate supercell in southwestern Barnes County around 0125 UTC, and caused nearly \$2 million in damage. The Barnes County tornado appeared considerably stronger than the F2 tornadoes further east when damage was surveyed in both areas at farmsteads that were in the path of the tornadoes. Some of

the most significant F4 damage can be seen in Fig. 3b and Fig. 3c. Satellite imagery, Fig. 4, shows the two supercells prior to the F4 tornado touchdown at 0125 UTC. The smaller supercell to the southwest, with a pronounced overshooting top, produced the violent tornado.

All tornadoes generally moved from north to south, with an average supercell storm motion of 360 degrees at  $9 \text{ m s}^{-1}$ . The F4 tornado was approximately 200 yards wide, and had a path length of 10 miles. Both F2 tornadoes had path lengths of 3 to 4 miles, and were approximately 100 yards wide. No injuries were reported with any of the tornadoes, however, at least 35 cows perished in the F4 tornado. As seen in Figs. 3b and 3c, damage to one farmstead by the F4 tornado was severe. Most structures in the direct path were totally destroyed.

### **3. Synoptic and mesoscale setting**

During the afternoon and evening of 18 July 2004, a ridge axis at 500 hPa (Fig. 5) extended from Colorado to Montana. At 300 hPa (not shown), a  $35 \text{ m s}^{-1}$  speed maximum propagated into the region. There was weak upper level diffluence over southeastern North Dakota around the time the tornadoes occurred. At 850 hPa (not shown), low-level moisture was relatively high over the Dakotas (dewpoints of  $17\text{-}20^\circ \text{ C}$ ), where there was relatively weak westerly flow.

Temperatures were  $+11^\circ \text{ C}$  or greater at 700 hPa (not shown) over much of North Dakota.

In the early afternoon at the surface, a pressure trough in central North Dakota moved slowly eastward. The trough was located just southeast of Jamestown, North Dakota (KJMS) by 0100 UTC (Fig. 6). A surface thermal ridge axis, with temperatures in excess of  $90^\circ \text{ F}$ , extended from near Bismarck, North Dakota (KBIS) to just east of KJMS. An axis of  $70\text{-}72^\circ \text{ F}$  surface dewpoints was oriented south to north over eastern North Dakota-perpendicular to the thermal ridge. These

dewpoints, likely aided by ET (to be discussed later in Section 5), enhanced instability where the highest surface temperatures were co-located with the highest dewpoints. Surface dewpoint depressions increased west of where the tornadic storms developed, with a dewpoint  $15^{\circ}\text{C}$  at KBIS at 2300 UTC. A very moist boundary layer, and the wind shift near the trough generated surface moisture flux convergence (not shown), contributing to upward low-level vertical motion over eastern North Dakota (Banacos and Schultz 2004).

#### **4. Environmental characteristics**

Instability on the evening of 18 July 2004 was large, and mixed-layer CAPE (MLCAPE) was around  $3000\text{ J kg}^{-1}$  (all mixed-layer computations in this paper use the mean mixing ratio and temperature of the lowest 100 hPa, similar to Thompson et al. (2003)). The 0000 UTC 19 July 2004 Eta model analysis in Fig. 7 indicated that MLCAPE was largest close to where the F4 tornadic storm developed. Although mixed-layer convective inhibition (MLCIN, not shown) was also large ( $-150$  to  $-200\text{ J kg}^{-1}$ ) over much of eastern North Dakota through most of the afternoon, heating and lift due to convergence along the surface trough initiated convection by late afternoon. Because convection developed, it is presumed that CIN was reduced sufficiently to allow initiation of several storms, including the violent tornadic supercell that intensified rapidly after 0000 UTC. When solar insolation ceased, all storms weakened quickly, suggesting that this event was driven largely by surface heating and low-level thermodynamics. The 0000 UTC 19 July 2004 observed sounding at Aberdeen, South Dakota (KABR, Fig. 8) confirmed that the environment to the south of the violent tornadic supercell was well capped, with MLCIN near  $-150\text{ J kg}^{-1}$ .

The 0-6-km shear as depicted on the early evening SPC mesoanalysis web page was strong over eastern North Dakota ( $> 25 \text{ m s}^{-1}$ , Fig. 9) and supportive of supercells (e.g., Rasmussen and Blanchard 1998; Thompson et al. 2003). In addition, the observed hodograph at KABR at 0000 UTC (Fig. 10) was relatively straight above 2 km, similar to long-lived supercell hodographs in Bunkers et al. (2006). The hodograph was also strongly clockwise curved in the lowest 2 km, which would favor cyclonic rotation of right-moving supercells (Rotunno and Klemp 1982). Based on estimated storm motions, the storm-relative helicity (SRH; Davies-Jones et al. 1990) in the 0-1 km layer from the KABR sounding was near  $150 \text{ m}^2\text{s}^{-2}$ . This is within the range associated with significant tornadoes (e.g., Rasmussen and Blanchard 1998; Thompson et al. 2003). Low-level storm-relative flow (SRF; Kerr and Darkow 1996) was also strong, and from the south ( $15 \text{ m s}^{-1}$  in the 0-1km layer). This suggested strong inflow to the supercells over eastern North Dakota from the unstable low-level air mass southeast of the surface trough.

Combinations of CAPE and SRH were large as well. Values of the energy-helicity index (EHI, Hart and Korotky 1991; Davies 1993) from the SPC mesoanalysis web page at 0000 UTC on 19 July 2004 (Fig. 11) were sizable over southeastern North Dakota ( $> 3.0$ ) based on 0-1 km SRH. This suggested statistical support for significant tornadoes (e.g., Rasmussen 2003; Thompson et al. 2003). Another useful severe weather forecast tool, based on operational experience at NWS Grand Forks, is the vorticity generation parameter (VGP, Rasmussen and Blanchard 1998). The VGP was large (0.4 to 0.7, not shown) on model analyses, also suggesting support for supercell tornadoes.

One environmental characteristic, the LCL height as depicted on the SPC 0000 UTC 19 July 2004 mesoanalysis (Fig. 2), did not appear particularly favorable prior to the development of the F4 tornado. Empirical statistical studies such as Rasmussen and Blanchard (1998), Thompson et

al. (2003), and Craven and Brooks (2004) have shown that most significant tornadoes are associated with mixed-layer LCL (MLLCL) heights below 1300-1500 m above ground. However, in this case, MLLCL heights from the SPC mesoanalysis at 0000 UTC (Fig. 2) were rather high, in the 1600-1800 m range. This will be examined later in section 6.

## **5. Potential effects of ET on low-level moisture and convective initiation**

Evapotranspiration (ET) frequently has important implications for convection initiation and subsequent storm strength. Raddatz (2000) showed that ET is a secondary (to advected moisture) but significant moisture source for the Canadian Prairie Provinces. ET also influences the timing and location of convection initiation (Hanesiak et al. 2004). Enhanced moisture, due to ET, raises CAPE values, which in turn increases the severity (Clark and Arritt 1995) of convection. Raddatz (1998) linked vegetative development and the seasonal pattern of ET to the annual pattern of convection. Raddatz and Cummine (2003) linked the peak occurrence of tornado days in the Canadian Prairie Provinces to the middle of the growing season when ET was greatest. These findings can be applied to the Northern Plains of the United States, which has a similar agroecosystem. Johns et al. (2000) suggested that ET plays a significant role in strong and violent tornado episodes across this region by increasing CAPE. Observational results (Segal et al. 1989) and numerical simulations (Chang and Wenzel 1991) have also suggested that convergence zones collocated with axes of enhanced boundary layer moisture are influenced by ET. It is important to note that axes of enhanced moisture along convergence zones can only occur when a local moisture source, such as ET is present.



The middle of the Northern Plains growing season and resultant increase in ET appeared to affect the 18 July 2004 case. Low-level moisture was under-forecast by most computer models, leading to an underestimation of convective potential at 0000 UTC 19 July 2004. As an example, the 1200 UTC 18 July 2004 Eta model run (Fig. 12a) indicated that regional surface dew points would rise to around 65°F during the afternoon of 18 July 2004. Instead, dewpoints near peak temperature time at 0000 UTC 19 July 2004 (Fig. 12b.) over eastern North Dakota increased to 70-73°F ahead of the surface trough. The fact that morning dewpoints (Fig. 12c) were only in the low to mid 60s (°F) over South Dakota, Nebraska, and Kansas with southerly surface winds across that area throughout the day implies that advection did not play a major role in raising dewpoints where the tornadoes occurred. It therefore appears that ET added moisture to the boundary layer during diurnal heating ahead of the surface trough, and was primarily responsible for increasing surface dewpoints over eastern North Dakota beyond levels forecast by operational models.

This enhanced low-level moisture increased CAPE, lowered CIN values, and likely affected convection initiation and intensity. Figure 13 shows an unmodified forecast sounding in Barnes County near the surface trough at 0000 UTC 19 July 2004 from the 1200 UTC Eta model. Figure 14 shows the same sounding modified in the lowest 1000 m based on observed surface observations. The lowest 1000m was randomly chosen for adjustment because this is similar to the lowest 100 hPa layer typically used in MLCAPE computations (e.g., Thompson et al. 2003). This modification increased MLCAPE from 1886 J kg<sup>-1</sup> to 3802 J kg<sup>-1</sup>, and reduced MLCIN from -46 J kg<sup>-1</sup> to -1 J kg<sup>-1</sup>. In addition, the 0-3-km MLCAPE (Rasmussen 2003) increased from 46 J kg<sup>-1</sup> to 160 J kg<sup>-1</sup>. This would imply stronger updrafts originating within the boundary layer.

The 1200 UTC 18 July 2004 Eta model forecast did not generate precipitation over eastern North Dakota. This was probably due in part to the large MLCIN that was forecast. However, with boundary layer moisture increased and MLCIN reduced due to ET, convergence along the trough was sufficient to initiate severe convection. The intensity of the thunderstorms that developed over North Dakota was probably influenced by the increased CAPE, which appeared to be enhanced by ET.

## **6. LCL height and low-level thermodynamic characteristics**

As noted in section 4, MLLCL heights in the Barnes County area (Fig. 2) where the F4 tornado developed appeared somewhat unfavorable (1600-1800 m above ground) for violent tornado development based on statistical research regarding supercell tornado environments. Furthermore, observed surface dewpoint depressions near the Barnes County area were around 10° C, a range suggested to be “nontornadic” by Markowski et al. (2002) when considering storm inflow and rear flank downdraft characteristics.

A recent study by Davies (2006a) suggests that many “high-LCL” tornadic environments combine very steep low-level lapse rates with low-level CAPE along with a level of free convection (LFC) not far above the LCL. Even with relatively high cloud bases (e.g., 1500-2000 m above ground), such a thermodynamic stratification would likely enhance parcel ascent within the lowest portion of the updrafts, with little, if any, low level CIN present. This might assist tornado development via low-level stretching before significant downdraft cold pools developed that could interfere with surface circulations beneath relatively high-based thunderstorms.

Notice that the model sounding in Fig. 14 that was modified to reflect observed surface moisture had important thermodynamic characteristics. The lapse rate below 2 km was steep (near super-adiabatic), and there was significant CAPE below 3 km. In addition, there was little CIN to inhibit rising mixed-layer parcels, and the LFC height was not far above the LCL. These characteristics were also shown by the SPC mesoanalysis over eastern North Dakota in the Jamestown area during the late afternoon of 18 July 2004. A southwest-to-northeast axis of very steep low-level lapse rates was evident by 2300 UTC (Fig. 15), impinging on an area of significant 0-3-km CAPE (Fig. 16). Figure 17 shows the overlap between these two fields two hours before the tornado formed, suggesting an environment that could enhance low-level stretching beneath cloud bases and within the lower portion of sustained updrafts.

As suggested in section 4, CAPE-shear characteristics over eastern North Dakota were already quite supportive of supercells and tornadoes on the evening of 18 July 2004. As explained in Davies (2006a), the addition of the low-level thermodynamic environment described above may have contributed to intense tornado development with the supercell over Barnes County. A violent tornado occurred even though LCL heights (Fig. 2) appeared noticeably higher than those in the vicinity of the larger diameter tornadic thunderstorm to the northeast.

## **7. Summary and conclusions**

Apart from LCL height, environmental parameters over North Dakota on the evening of 18 July 2004,, such as SRH, deep-layer shear, and CAPE-shear combinations, were quite supportive of supercell tornadoes based on recent research. The strongest tornado of this event, rated F4, formed with a supercell that developed in a high-LCL environment well to the west of a larger

supercell that produced weaker tornadoes associated with somewhat lower LCL heights.

Although it is not possible to claim a role for environmental variability in governing the intensity of tornadoes on a given day *within a small region*, it is worth noting that the F4 tornadic thunderstorm formed in an area of maximum surface temperature and dewpoints, resulting in considerable instability. MLCAPE for this event was quite large (around  $3000 \text{ J kg}^{-1}$ ), similar to findings in Davies (2006b) that showed large values of MLCAPE to be associated with significant tornado cases where LCL heights are relatively high. The fact that low-level lapse rates were also maximized and co-located with relatively large low-level MLCAPE values along the surface trough and wind shift boundary (discussed in section 6) may have had an additional affect on tornado intensity via enhanced stretching, in spite of the high LFC height.

It should be emphasized that prior studies regarding tornadoes and LCL heights have been statistical in nature, and were likely biased toward the eastern United States and lower ground elevations, where higher F-scale ratings are easier to garner due to higher population density and more structures. Similar to cases in Davies (2006a and 2006b), this event is a reminder that LCL height as a “limiting factor” should be used with caution, especially when other thermodynamic and kinematic factors appear quite favorable for supercells and tornadoes. Future research, including storm modeling and scientific field observations, needs to focus on the physics of the role of low-level stability regarding tornadic supercells, including environments with relatively high LCL heights.

The supercell that eventually produced the F4 tornado was relatively small in size compared to the other tornadic supercell during this event (Fig. 18). The larger supercell appeared more “classic” on radar (larger size, hook echo “appendage”, outflow boundary, etc. as discussed by Lemon and Doswell (1979)) than the smaller, younger supercell to the southwest, yet it produced

weaker tornadoes. This reaffirms that there is not necessarily an association between radar size/appearance of a supercell and the intensity of tornadoes produced. This case demonstrates that a relatively small and newly developed supercell can produce strong or violent tornadoes if the local environment is favorable.

Evapotranspiration (ET), discussed in section 5, likely had an impact on the storm environment. Moisture added to the boundary layer ahead of the surface trough by ET appeared responsible for enhanced surface dewpoints over eastern North Dakota that were not forecast by operational models. Because this added moisture likely affected convective initiation and intensity, this case appears to emphasize the importance of ET as a factor that forecasters need to consider when making thunderstorm forecasts during the growing season.

Presenting several operational challenges, the authors believe this case serves as an example of several localized factors coming together to generate a violent tornado. The recognition of certain environmental variables, such as enhanced moisture and surface heating along a slow moving boundary near the periphery of a capping inversion should suggest heightened situational awareness for severe weather forecasters. In such cases, though LCL heights may appear relatively high in a statistical sense (e.g., 1500-2000 m), favorable CAPE and shear parameters in combination with the presence of steep low-level lapse rates may signal potential for significant supercell tornado development.

### *Acknowledgements*

The authors would like to thank Bradley Bramer (NWS Grand Forks, ND) for providing his review, comments, and valuable suggestions on the manuscript. The authors would also like to thank Matt Bunkers (NWS Rapid City, SD) for providing images from his sounding and

hodograph programs, along with his insight and review of an early version of this paper. The authors would like to thank Joshua Smith for working on the damage analysis of this tornado, and providing input on this case study. Jared Guyer (SPC) is gratefully acknowledged for providing SPC mesoanalysis images. The authors would also like to thank Erik Rasmussen (CIMMS), and 2 anonymous reviewers for their careful review, suggestions and insight to the manuscript. Lastly, the authors would like to thank Rick Hozak and Mark Ewens (NWS Grand Forks, ND) for their help and assistance in creating many of the images in this paper.

## References

- Banacos, P. C., and D. M. Schultz, 2004: The use of moisture flux convergence in forecasting convective initiation: Historical and operational perspectives. *Wea. Forecasting*, **20**, 351-366.
- Bothwell, P. D., J. A. Hart, and R. L. Thompson, 2002: An integrated three-dimensional objective analysis scheme in use at the Storm Prediction Center. Preprints, *21<sup>st</sup> Conf. on Severe Local Storms*, San Antonio, TX, Amer. Meteor. Soc., J117-J120.
- Bunkers, M. J., J. S. Johnson, L. J. Czepyha, J. M. Grzywacz, B. A. Klimowski, and M. R. Hjelmfelt, 2006: An observational examination of long-lived supercells. Part II: Environmental conditions and forecasting. *Wea. Forecasting*, in press.
- Chang, J. and P. J. Wetzel, 1991: Effects of spatial variations of soil and vegETAtion on the evolution of a prestorm environment: A numerical case study. *Mon. Wea Rev.*, **119**, 1368-1390.
- Clark, C. A. and R. W. Arritt, 1995: Numerical simulation of the effect of soil moisture and vegETAtion cover on the development of deep convection. *J. Appl. Meteor.*, **34**, 2029-2045.
- Craven, J. P., and H. E. Brooks, 2004: Baseline climatology of sounding-derived parameters associated with deep moist convection. *Natl. Wea Dig.*, **28**, 13-24.
- Davies, J. M., 1993: Hourly helicity, instability, and EHI in forecasting supercell tornadoes. Preprints, *17<sup>th</sup> Conf. on Severe Local Storms*, St. Louis, MO, Amer. Meteor. Soc., 107-111.
- , 2006a: Tornadoes in environments with small helicity and/or high LCL heights. *Wea. Forecasting*, **21**, 579-594.

- , 2006b: Total CAPE, low-level CAPE, and LFC in significant tornado events with relatively high LCL heights. Preprints, *23<sup>rd</sup> Conf. on Severe Local Storms*, St. Louis, MO, Amer. Meteor. Soc., CD-ROM, P1.3.
- , and R. H. Johns, 1993: Some wind and instability parameters associated with strong and violent tornadoes. 1. Wind shear and helicity. *The Tornado: Its Structure, Dynamics, Prediction, and Hazards, Geophys. Monogr.*, No. 79, Amer. Geophys. Union, 573-582.
- Davies-Jones, R. P., D. Burgess, and M. Foster, 1990: Test of helicity as a tornado forecast parameter. Preprints, *16<sup>th</sup> Conf. on Severe Local Storms*, Kananaskis Park, AB, Canada, Amer. Meteor. Soc., 588-592.
- Hanesiak, J. M., R. L. Raddatz, S. Lobban, 2004: Local initiation of deep convection on the Canadian prairie provinces. *Bound.-Layer Meteor.*, **110**, 455-470.
- Hart, J. A., and W. Korotky, 1991: The SHARP workstation v1.50 users guide. NOAA/National Weather Service. 30 pp. [Available from NWS Eastern Region Headquarters, 630 Johnson Ave., Bohemia, NY 11716.]
- Holt, Teddy R., D. Niyogi, F. Chen, K. Manning, M. A. LeMone, and A. Qureshi, 2006: Effect of Land–Atmosphere Interactions on the IHOP 24–25 May 2002 Convection Case. *Mon. Wea. Rev.*, **134**, 113–133.
- Johns, R. H., C. Broyles, D. Eastlack, H. Guerrero and K. Harding, 2000: The role of synoptic patterns and moisture distribution in determining the location of strong and violent tornado episodes in the north central United States: A preliminary examination. Preprints, *20<sup>th</sup> Conference on Severe Local Storms.*, Orlando, FL, 489-492.
- Kerr, B. W., and G. L. Darkow, 1996. Storm-relative winds and helicity in the tornadic thunderstorm environment. *Wea Forecasting*, **11**, 489-505.



- Lemon, L. R., and C. A. Doswell III, 1979: Severe thunderstorm evolution and mesocyclone structure as related to tornadogenesis. *Mon. Wea. Rev.*, **107**, 1184-1197.
- Markowski, P. M., J. M. Straka, and E. N. Rasmussen, 2002: Direct surface thermodynamic observations within rear-flank downdrafts of nontornadic and tornadic supercells. *Mon. Wea. Rev.*, **130**, 1692-1721.
- Raddatz, R. L., 1998: Anthropogenic vegetation transformation and the potential for deep convection on the Canadian prairies. *Can. J. Soil. Sci.*, **78**, 656-666.
- , 2000: Summer rainfall recycling for an agricultural region of the Canadian prairies. *Can. J. Soil. Sci.*, **80**, 367-373.
- , and J. D. Cummine, 2003: Inter-annual variability of moisture flux from the prairie agro-ecosystem: Impact of crop phenology on the seasonal pattern of tornado days. *Bound.-Layer Meteor.*, **106**, 283-295.
- Rasmussen, E. N., 2003: Refined supercell and tornado forecast parameters. *Wea. Forecasting*, **18**, 530-535.
- , and D. O. Blanchard, 1998: A baseline climatology of sounding-derived supercell and tornado forecast parameters. *Wea. Forecasting*, **13**, 1148-1164.
- Rotunno, R. and J. B. Klemp, 1982: The influence of the shear-induced pressure gradient on thunderstorm motion. *Mon. Wea. Rev.*, **110**, 136-151.
- Segal M., W. E. Schreiber, G. Kallos, J. R. Garratt, A. Rodi, J. Weaver, and R. A. Pielke, 1989: The impact of crop areas in northeast Colorado on midsummer mesoscale thermal circulations. *Mon. Wea. Rev.*, **117**, 809-825.

Thompson, R. L., J. A. Edwards, A. Hart, K. L. Elmore and P. Markowski, 2003: Close Proximity Soundings within supercell environments obtained from the Rapid Update Cycle. *Wea. Forecasting*, **18**, 1243-1261.

### Figure Captions

Figure 1. Tornado (F4 intensity) with relatively high-based supercell cloud base ( $> 1600$  m AGL) over southwest Barnes County, North Dakota, around 0130 UTC on 19 July 2004. View is to the north. Photographer unknown.

Figure 2. SPC mesoanalysis of mixed-layer LCL height (m AGL, contour spacing 200 m) at 0000 UTC 19 July 2004. Location of F4 tornado at 0125 UTC is denoted by a solid inverted triangle.

Figure 3a. Map of tornado tracks over eastern North Dakota on the evening of 18-19 July 2004. Bold line marks Eastern North Dakota NWS county warning area. Corresponding letters shown in inset box indicate initial touchdown times and F-scale intensities. County boundaries are also shown. Tornadoes A-D and F-H were spawned by one large supercell. Tornado 'E' was spawned from a separate and smaller supercell storm.

Figure 3b. F4 damage to a farmstead in southwestern Barnes County, North Dakota, from the

violent tornado. Photo by Mark Ewens.

Figure 3c. Debris pile from the violent tornado at the same farmstead as in Fig 3b. The bent steel I-beam on top indicates F4 damage. Photo by Mark Ewens.

Figure 4. GOES-12 visible satellite imagery at 0045 UTC 19 July 2004, with tornadic supercells indicated by arrows. The smaller supercell to the southwest produced the destructive F4 tornado 40 minutes later.

Figure 5. 500 hPa analysis at 0000 UTC on 19 July 2004 with observations (conventional) also shown. Solid lines are geopotential height, with a contour interval of 6 dam.

Figure 6. Surface observations (conventional, ° F) at 0100 UTC on 19 July 2004 over eastern North Dakota, northeastern South Dakota, and northwestern Minnesota. Solid contours are surface isobars analyzed at 1-hPa intervals. Surface pressure trough is indicated by heavy dashed line. Location of F4 tornado at 0125 UTC 19 July 2004 is denoted by solid inverted triangle.

Figure 7. Eta initial analysis field of MLCAPE (solid contours, intervals of  $200 \text{ J kg}^{-1}$ ) at 0000 UTC 19 July 2004, using the lowest 100-hPa mixed-layer lifted parcels. Location of the F4 tornado shown as in Fig. 6.

Figure 8. SkewT-logp diagram of observed sounding at Aberdeen, South Dakota at 0000 UTC 19 July 2004. Heavy solid black line is the environmental temperature profile. Heavy solid gray line is the dewpoint profile, and the heavy dotted black line is lifted parcel trace above LFC based on

the lowest 100-hPa mixed layer parcel. Wind vector lines showing speed (kts) and direction orientation are in gray at right. Heights are given in km AGL.

Figure 9. SPC mesoanalysis of 0-6-km shear (solid contours  $\geq 30$  kts, 5 kt intervals) at 0000 UTC 19 July 2004. Wind barbs (conventional) denote shear value at evenly spaced locations. Location of the F4 tornado shown as in Fig. 2.

Figure 10. Ground-relative hodograph at 0000 UTC 19 July 2004 from observed winds in Fig. 8. Each background ring represents  $5 \text{ m s}^{-1}$  (10 kts).  $V_{\text{obs}}$  indicates observed storm motion from F4 tornadic storm.

Figure 11. As in Fig. 9, except 0-1-km energy-helicity index parameter (solid contours  $\geq 1$ , Non-dimensional with spacing of 1).

Figure 12a. Forecast field of dewpoint ( $^{\circ}$  F,  $5^{\circ}$  F spacing) at 0000 UTC 19 July 2004 from 1200 UTC 18 July 2004 Eta model.

Figure 12b. Analysis field of dewpoint ( $^{\circ}$  F,  $5^{\circ}$  F spacing) at 0000 UTC 19 July 2004.

Figure 12c. Analysis field of dewpoint ( $^{\circ}$  F,  $5^{\circ}$  F spacing) at 1200 UTC 18 July 2004.

Figure 13. As in Fig. 8, except Eta 12-hr forecast sounding in southwestern Barnes County, North Dakota valid at 0000 UTC 19 July 2004 near the location of the F4 tornado.

Figure 14. Same profile as in Fig. 14, except modified to reflect enhanced moisture in the lowest 1000 m based on observed surface dewpoints ( $3.5\text{ }^{\circ}\text{C}$  greater than forecast in Fig. 13).

Figure 15. SPC mesoanalysis of 0-3-km lapse rate ( $^{\circ}\text{C km}^{-1}$  at  $0.5^{\circ}\text{C}$  spacing) at 2300 UTC 18 July 2004. Axis of steepest low-level lapse rates indicated by dots. Location of the F4 tornado shown as in Fig. 2.

Figure 16. As in Fig. 15, except 0-3-km CAPE (thick solid lines  $\geq 25\text{ J kg}^{-1}$ ,  $25\text{ J kg}^{-1}$  spacing) and surface vorticity (thin lines,  $10^{-4}\text{ s}^{-1}$ ). Surface wind barbs (conventional) are also shown.

Figure 17. As in Fig. 15, except area where 0-3-km lapse rates  $\geq 8^{\circ}\text{C km}^{-1}$  overlap 0-3-km CAPE  $\geq 25\text{ J kg}^{-1}$  from Fig. 16.

Figure 18. Mayville, ND WSR-88D (KMVX) base reflectivity at 0144 UTC 19 July 2004. The supercell producing the F4 tornado at the time of this image is indicated by the white arrow.



Fig. 1. Tornado (F4 intensity) with relatively high-based supercell cloud base ( $> 1600$  m AGL) over southwest Barnes County, North Dakota, around 0130 UTC on 19 July 2004. View is to the north. Photographer unknown.

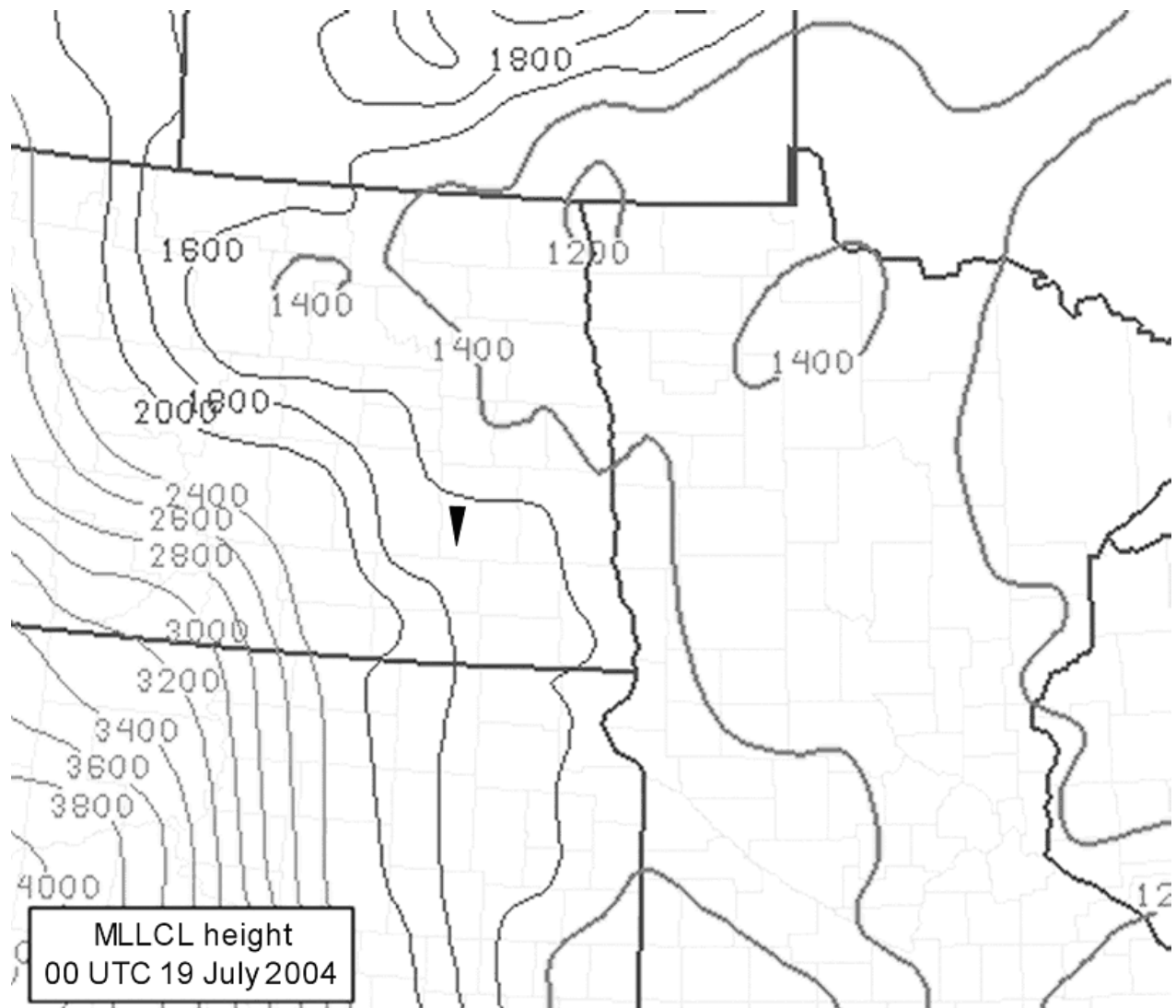


Fig. 2. SPC mesoanalysis of mixed-layer LCL height (m AGL, contour spacing 200 m) at 0000 UTC 19 July 2004. Location of F4 tornado at 0125 UTC is denoted by solid inverted triangle.

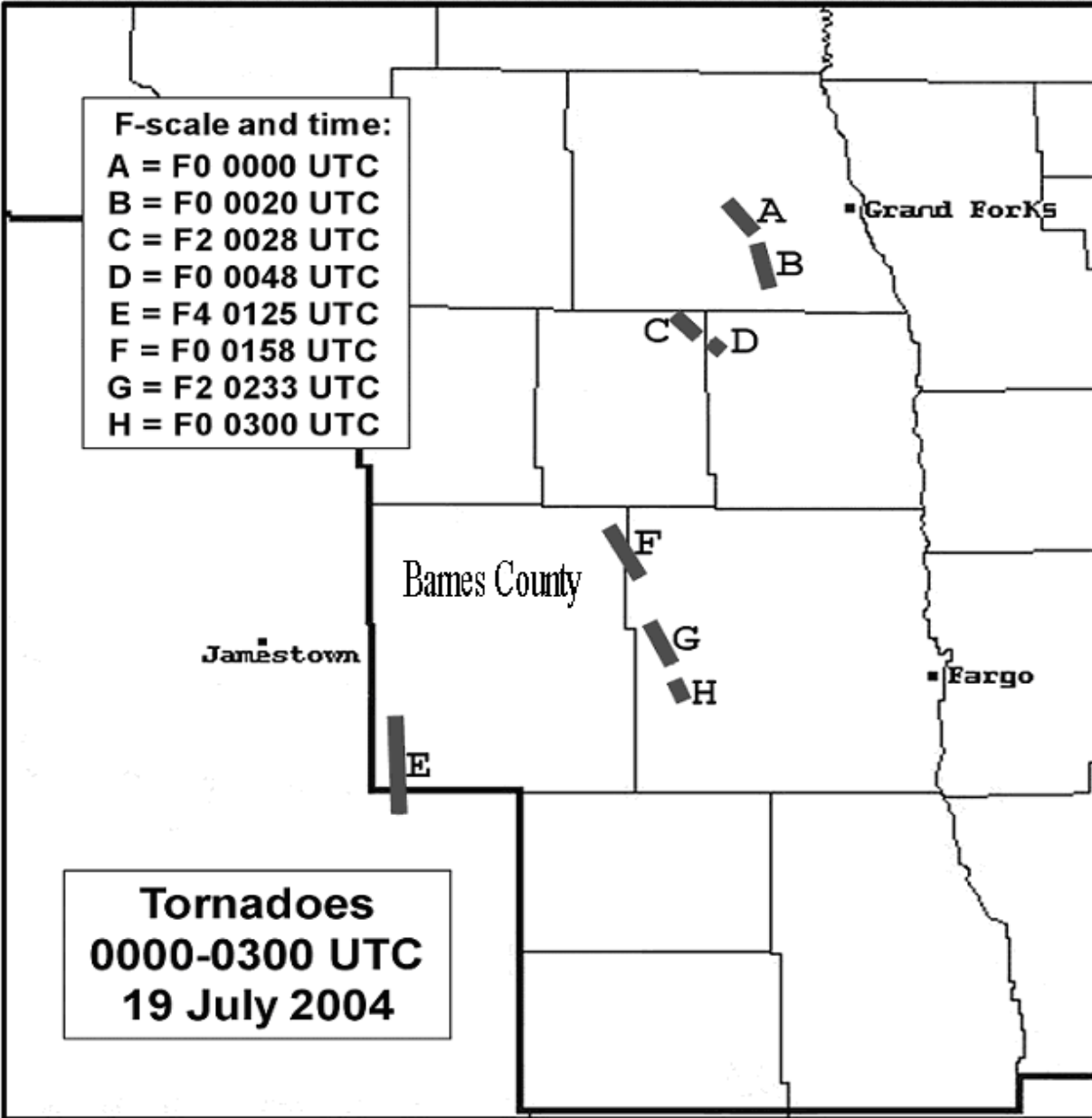


Fig. 3a. Map of tornado tracks over eastern North Dakota on the evening of 18-19 July 2004. Bold line marks Eastern North Dakota NWS county warning area. Corresponding letters shown in inset box indicate initial touchdown times and F-scale intensities. County boundaries are also shown. Tornadoes A-D and F-H were spawned by one large supercell. Tornado 'E' was spawned from a separate and smaller supercell storm.





Fig. 3b. F4 damage to a farmstead in southwestern Barnes County, North Dakota, from the violent tornado. Photo by Mark Ewens.



Fig. 3c. Debris pile from the violent tornado at the same farmstead as in Fig 3a. The bent steel I-beam on top indicates F4 damage. Photo by Mark Ewens.

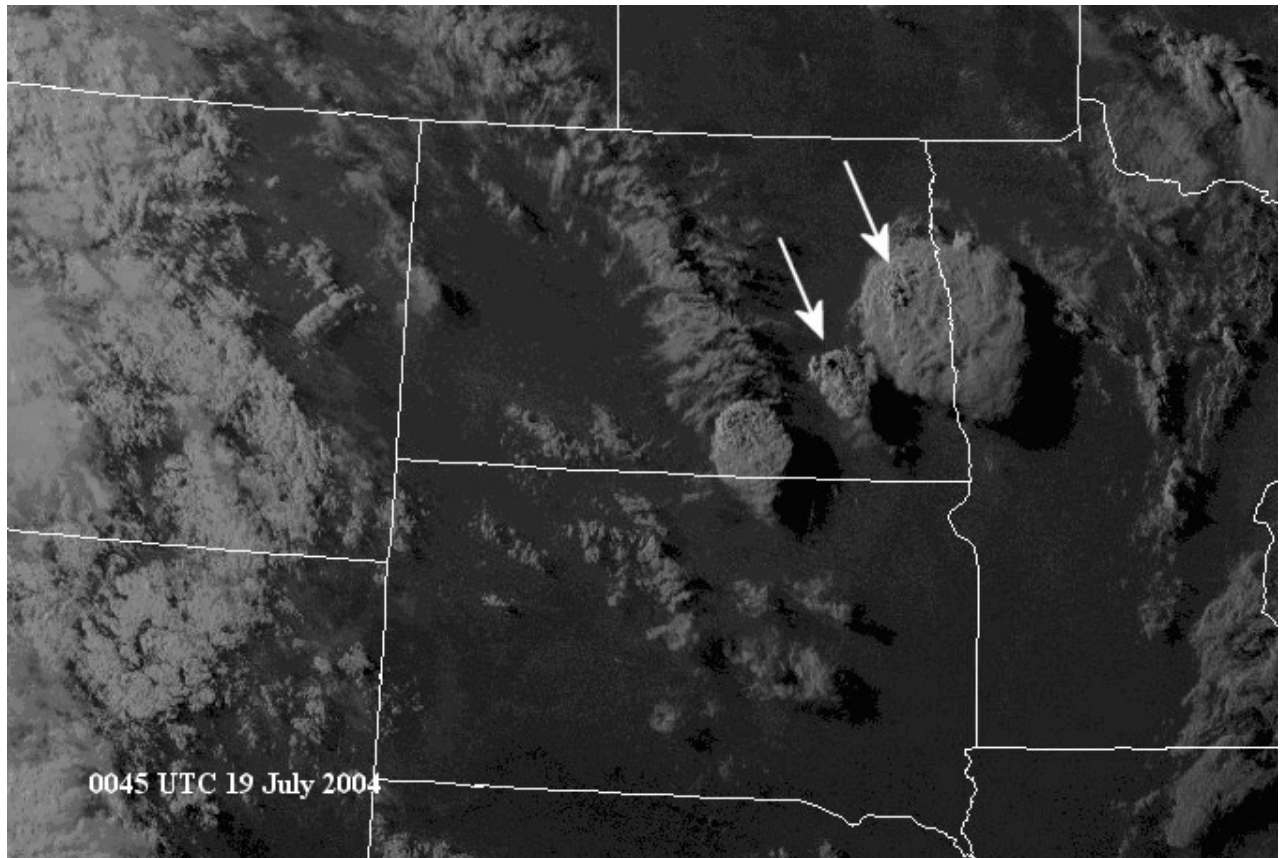


Fig. 4. GOES-12 Visible satellite imagery at 0045 UTC 19 July 2004, with tornadic supercells indicated by arrows. The smaller supercell to the southwest produced the destructive F4 tornado 40 minutes later.

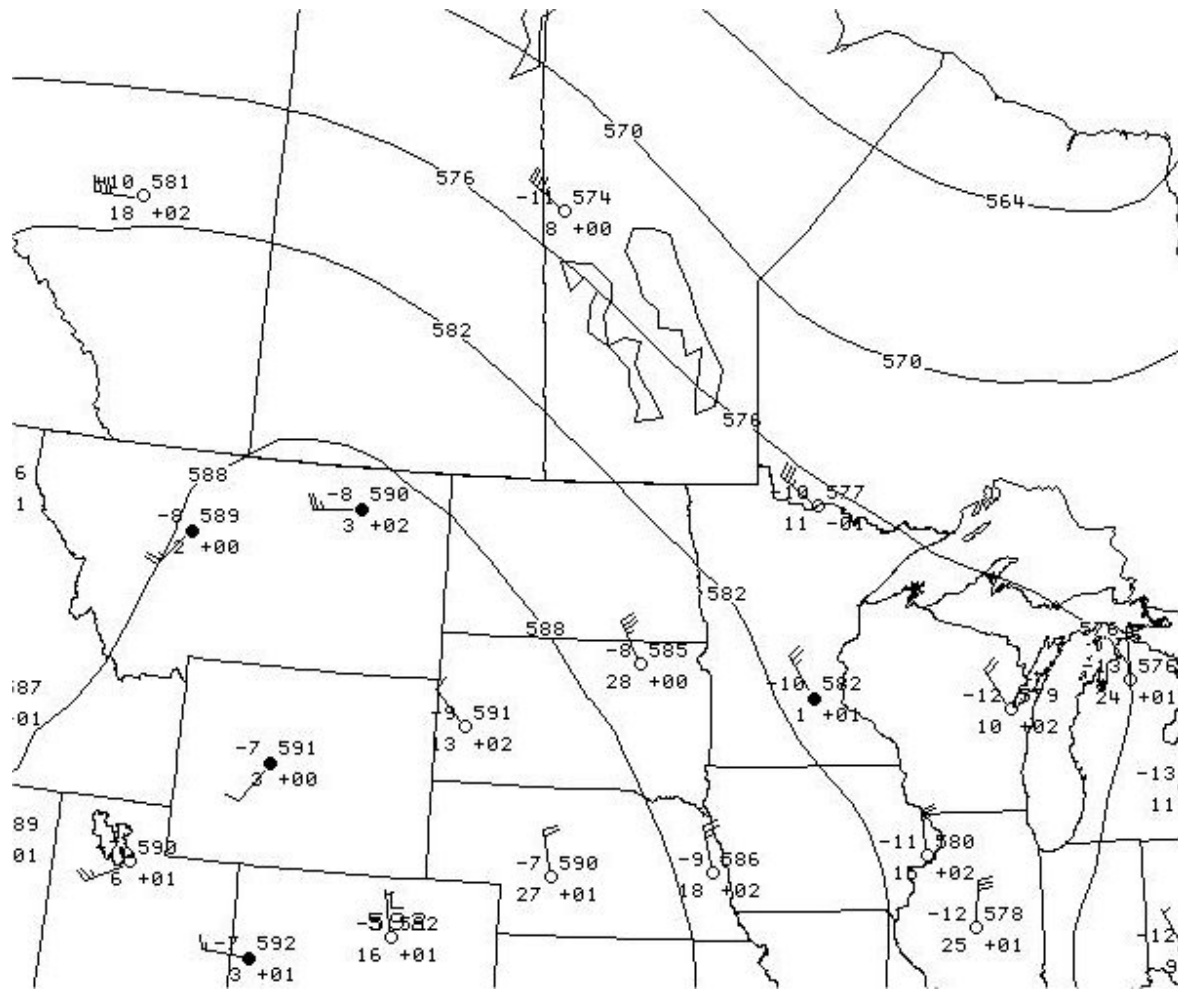


Fig. 5. 500 hPa analysis at 0000 UTC on 19 July 2004 with observations (conventional) also shown. Solid lines are geopotential height, with a contour interval of 6 dam.



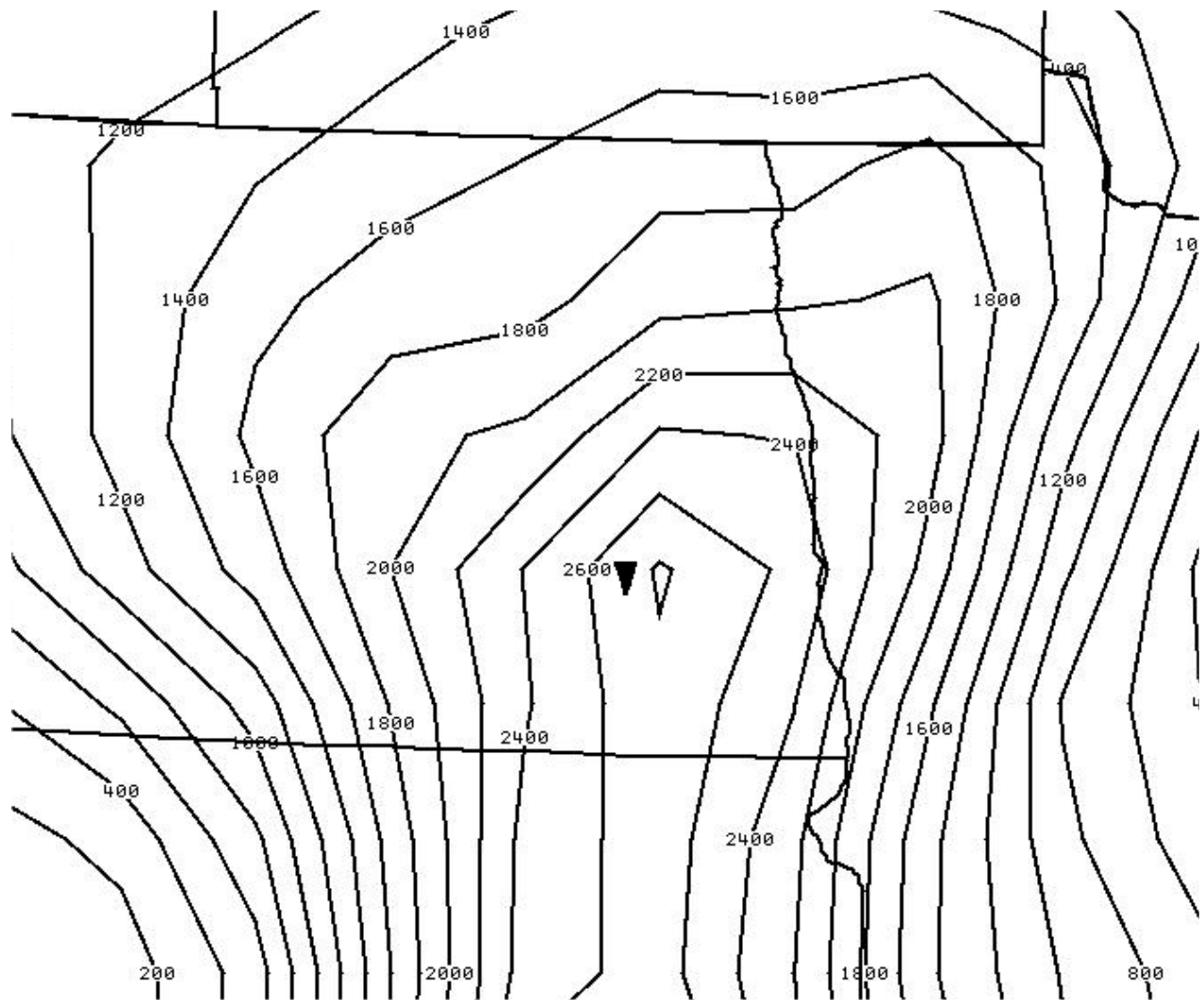


Fig. 7. Eta initial analysis field of MLCAPE (solid contours, intervals of  $200 \text{ J kg}^{-1}$ ) at 0000 UTC 19 July 2004, using the lowest 100-hPa mixed-layer lifted parcels. Location of the F4 tornado shown as in Fig. 2.

ABR 0000 UTC 19 July 2004

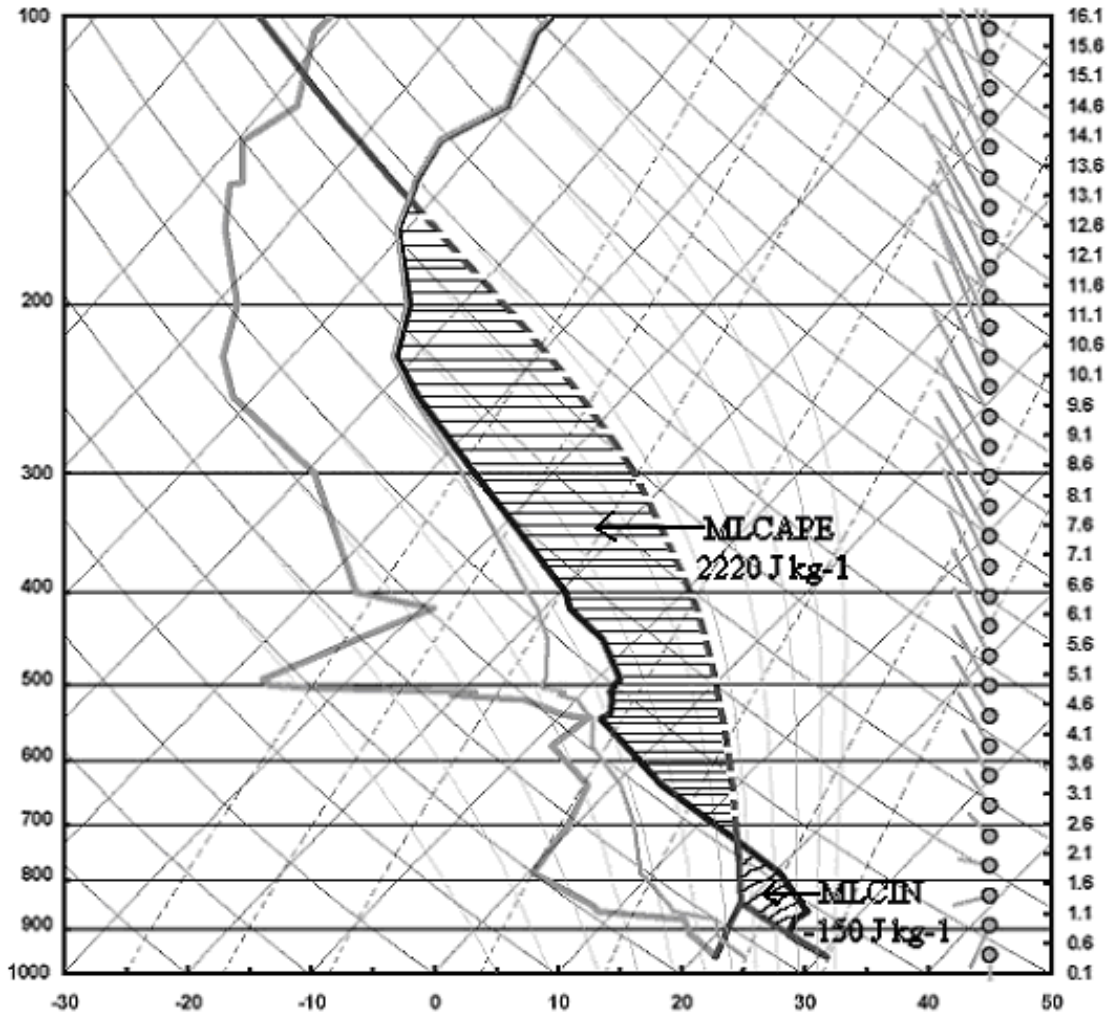


Fig. 8. Skew $T$ -log $p$  diagram of observed sounding at Aberdeen, South Dakota at 0000 UTC 19 July 2004. Heavy solid black line is the environmental temperature profile. Heavy solid gray line is the dewpoint profile, and the heavy dotted black line is lifted parcel trace above LFC based on the lowest 100-hPa mixed layer parcel. Wind vector lines showing speed (kts) and direction orientation are in gray at right. Heights are given in km AGL.

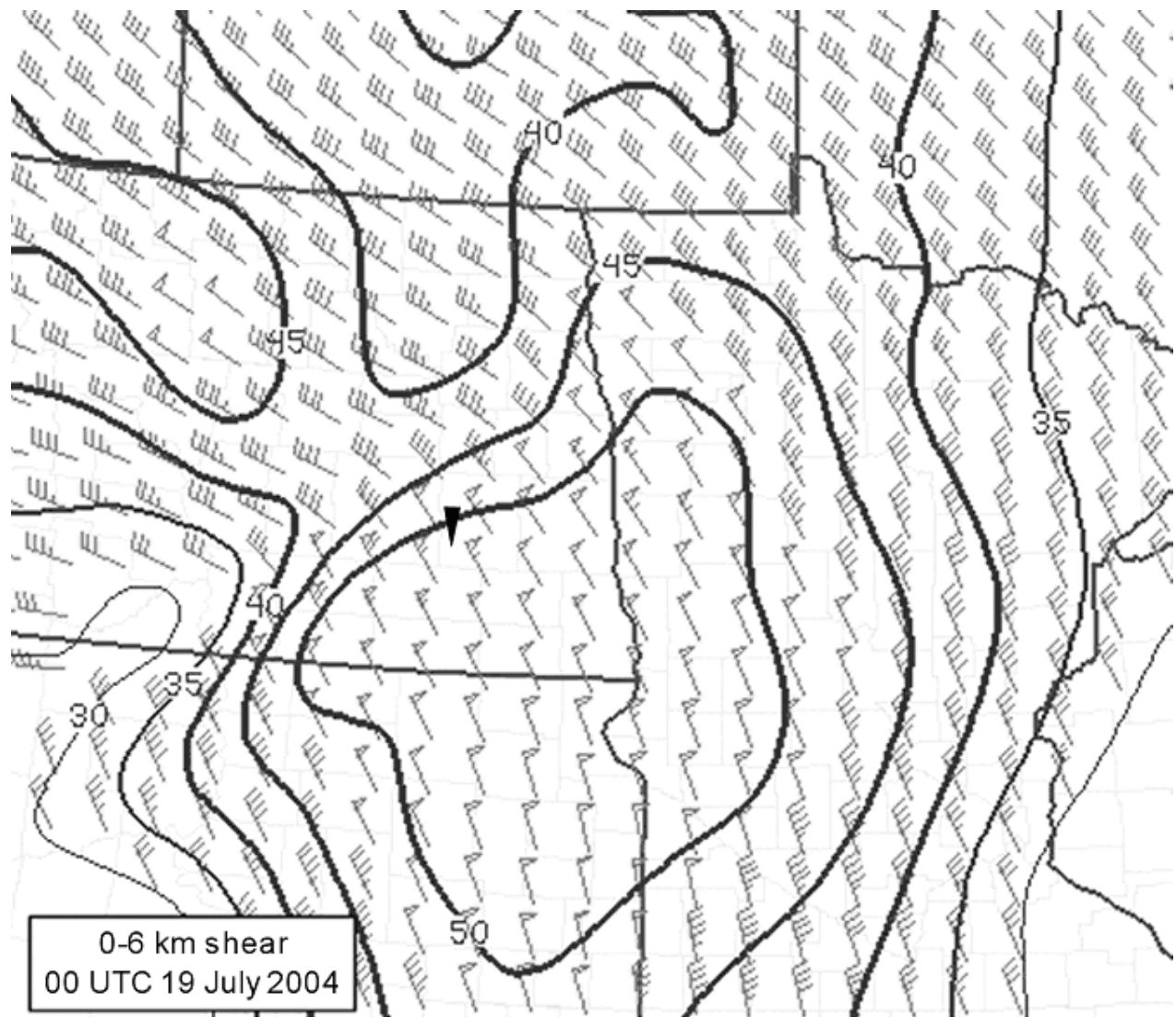


Fig. 9. SPC mesoanalysis of 0-6-km shear (solid contours  $\geq 30$  kts, 5 kt interval) at 0000 UTC 19 July 2004. Wind barbs (conventional) denote shear value at evenly spaced locations. Location of the F4 tornado shown as in Fig. 2.

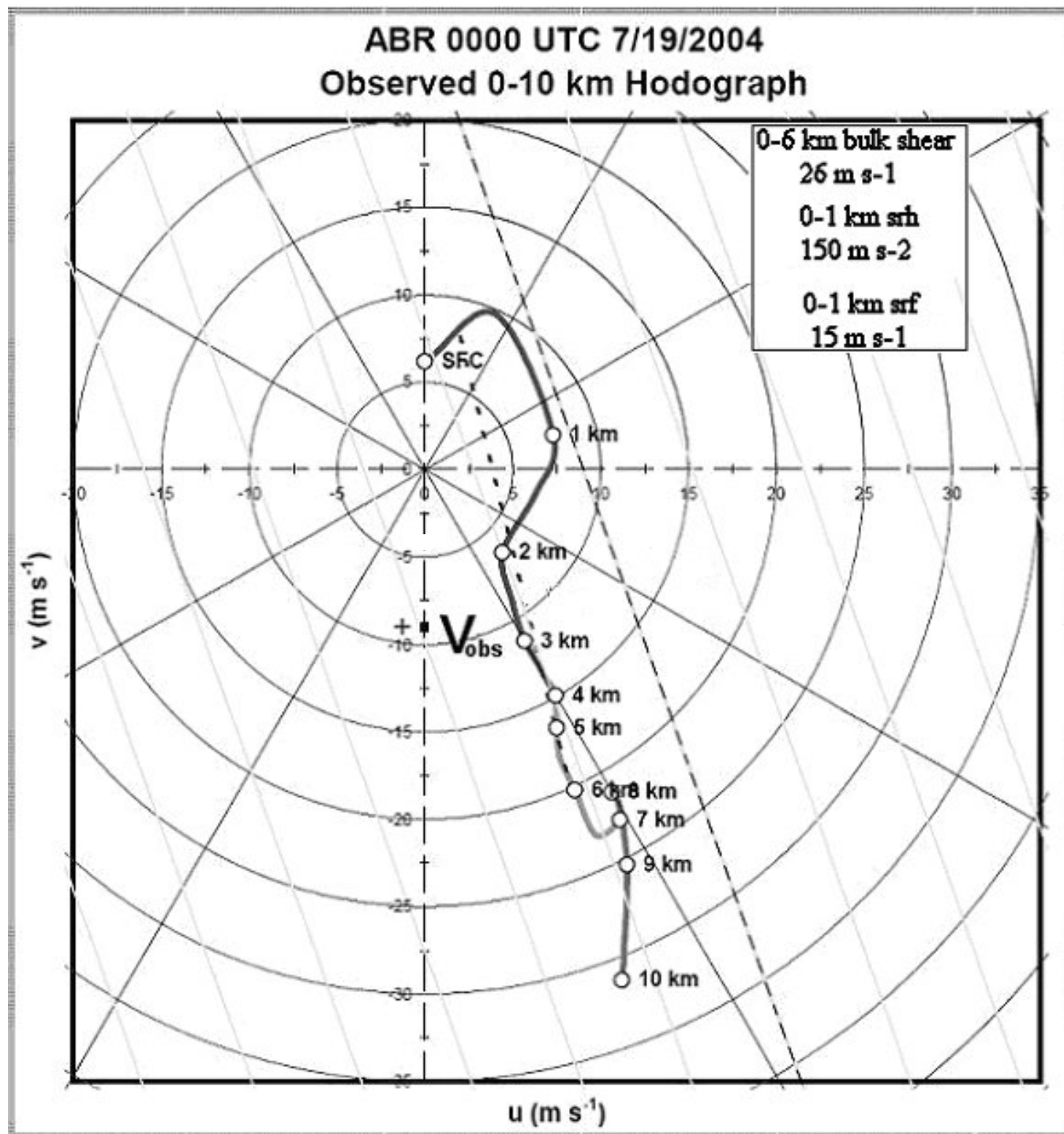


Fig. 10. Ground-relative hodograph at 0000 UTC 19 July 2004 from observed winds in Fig. 8.

Each background ring represents 5 m s<sup>-1</sup> (10 kts).  $V_{obs}$  indicates observed storm motion from F4 tornadic storm.



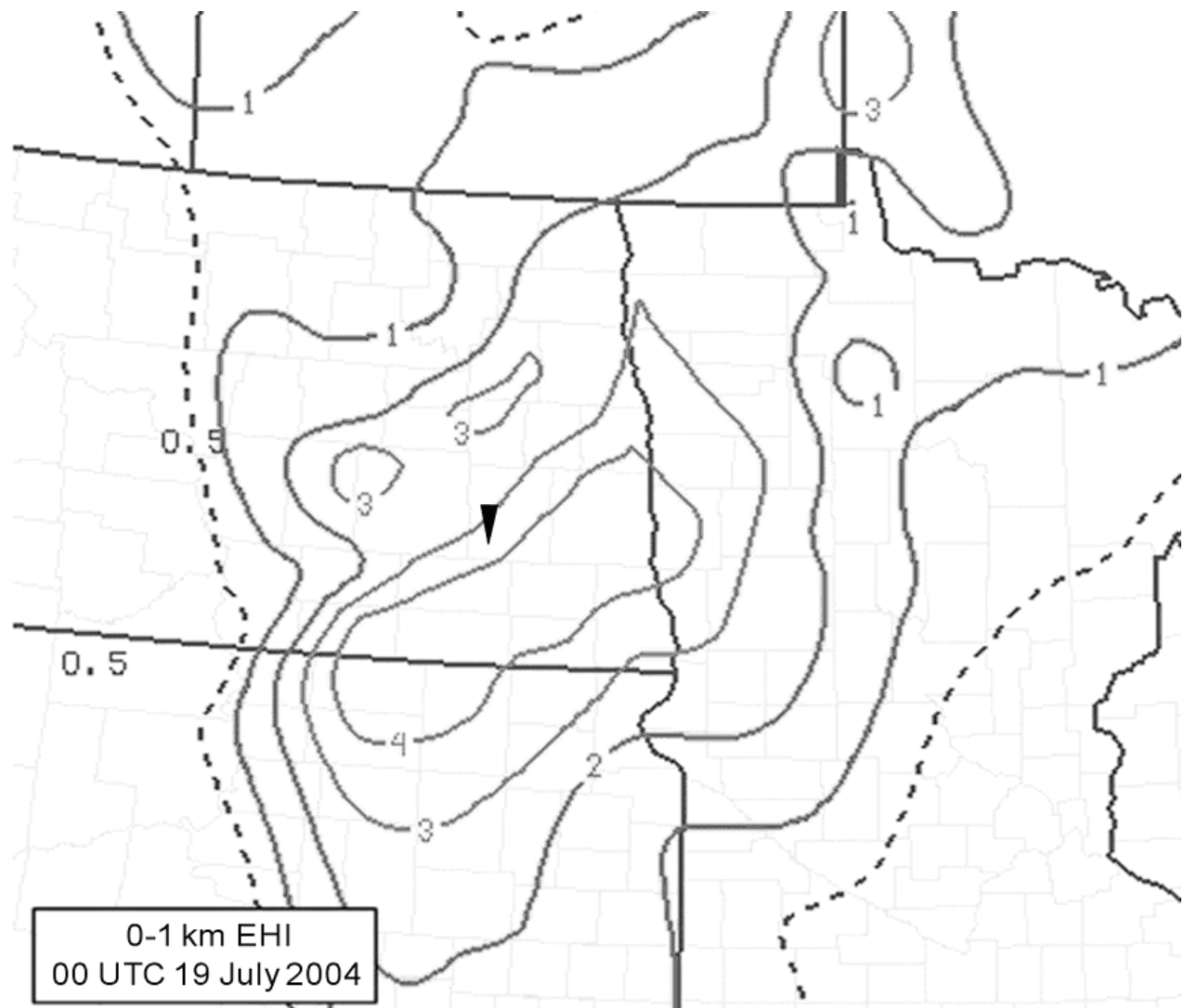


Fig. 11 As in Fig. 9, except 0-1-km energy-helicity index parameter (solid contours  $\geq 1$ , Non-dimensional with spacing of 1).

1200 UTC 18 July 2004 ETA model  
valid at 0000 UTC 19 July 2004

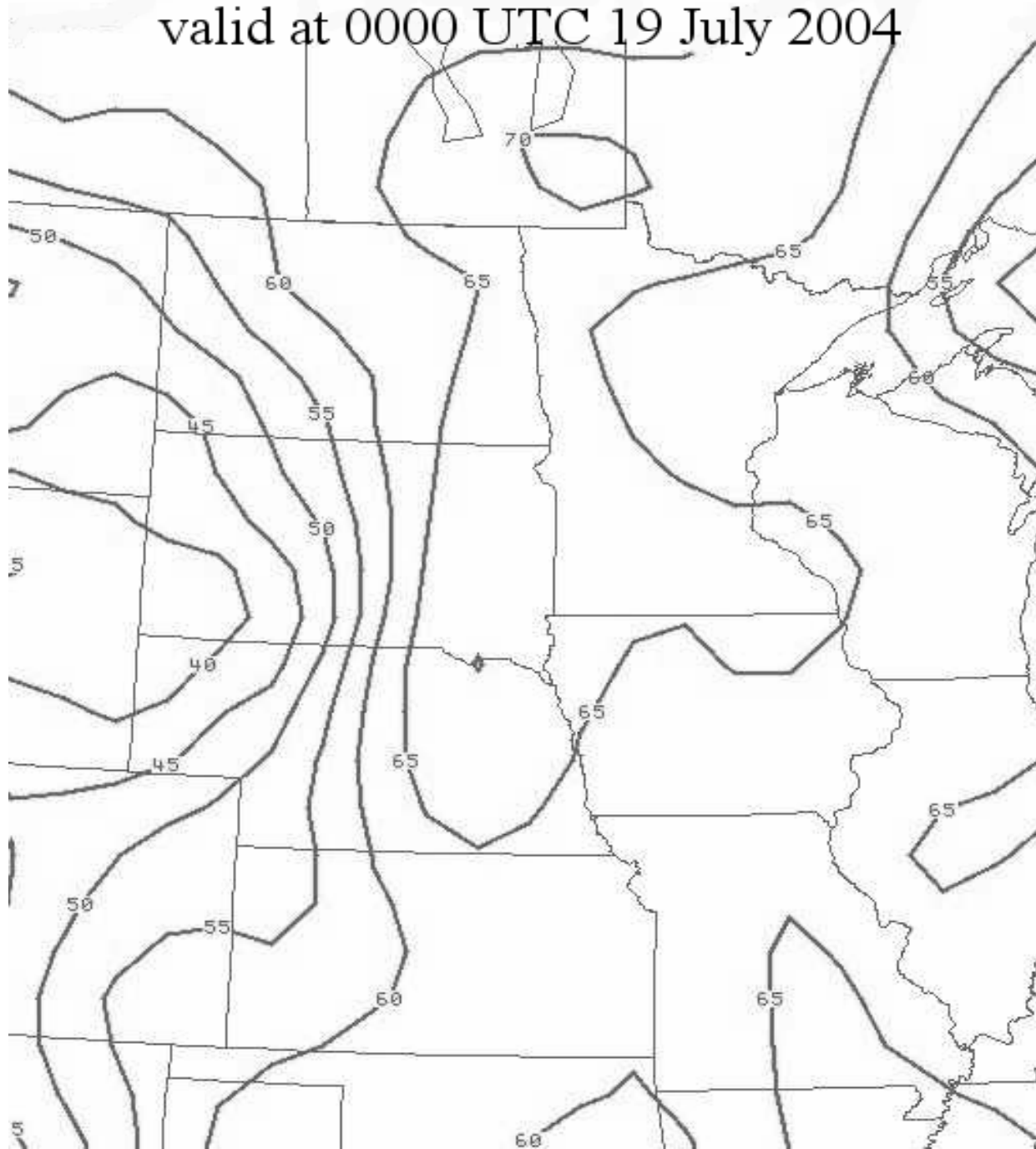


Fig. 12a. Forecast field of dewpoint ( $^{\circ}$  F,  $5^{\circ}$  F spacing) at 0000 UTC 19 July 2004 from 1200 UTC 18 July 2004 Eta model.

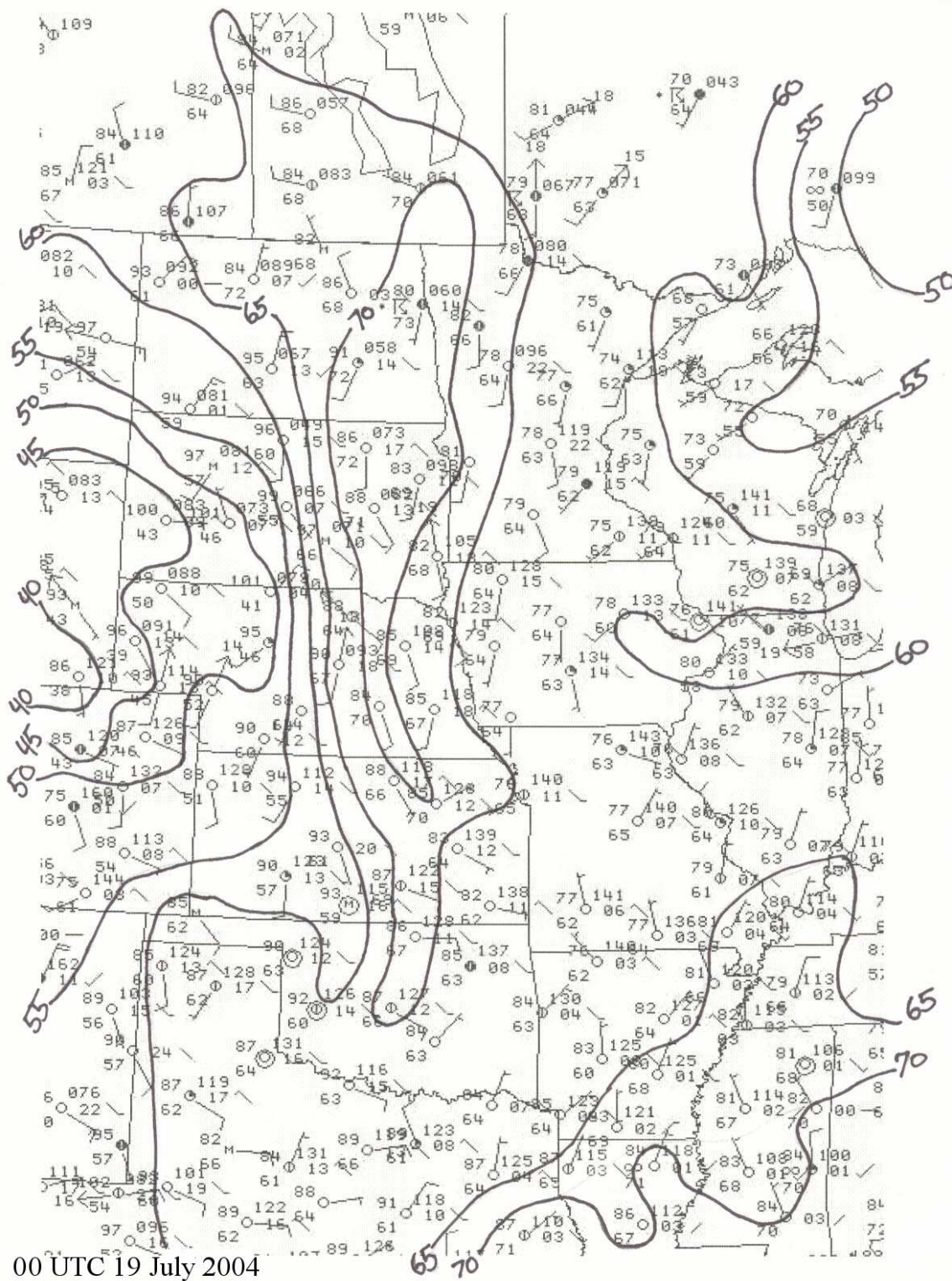


Fig. 12b. Analysis field of dewpoint ( $^{\circ}$  F,  $5^{\circ}$  F spacing) at 0000 UTC 19 July 2004.

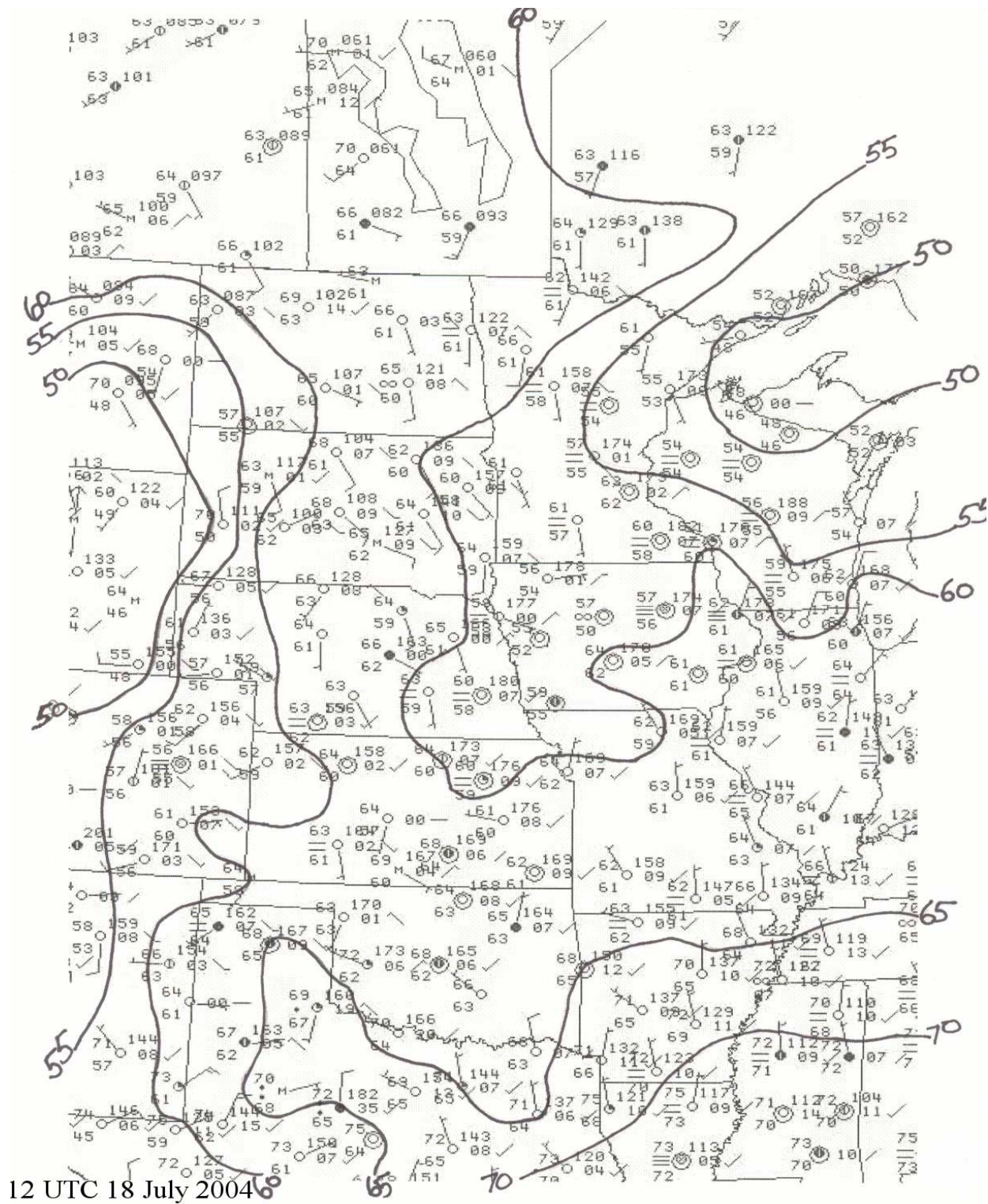


Fig. 12c. Analysis field of dewpoint ( $^{\circ}$  F,  $5^{\circ}$  F spacing) at 1200 UTC 18 July 2004.

12zEtarun\_00zJuly19

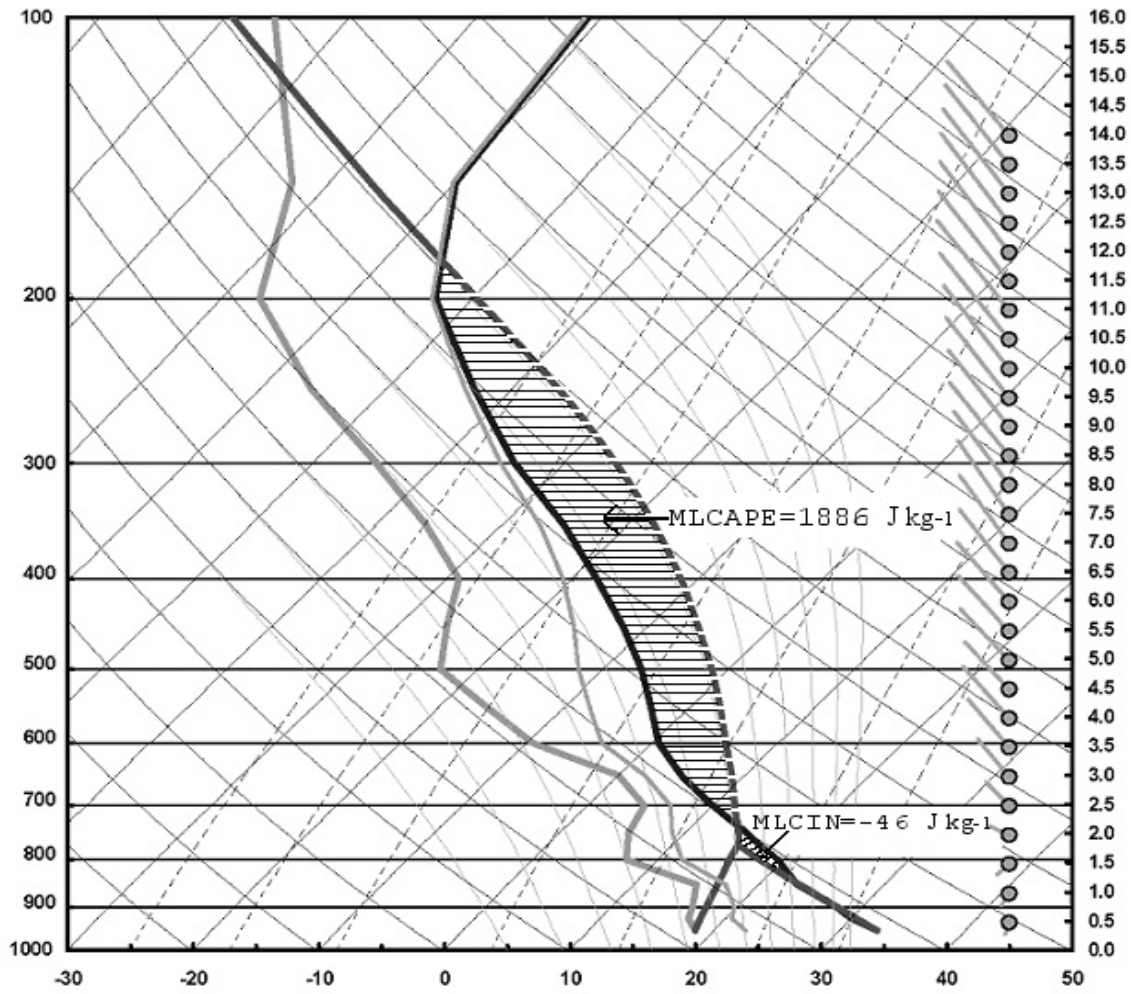


Fig. 13. As in Fig. 8, except Eta 12-hr forecast sounding in southwestern Barnes County, North Dakota valid at 0000 UTC 19 July 2004 near the location of the F4 tornado.

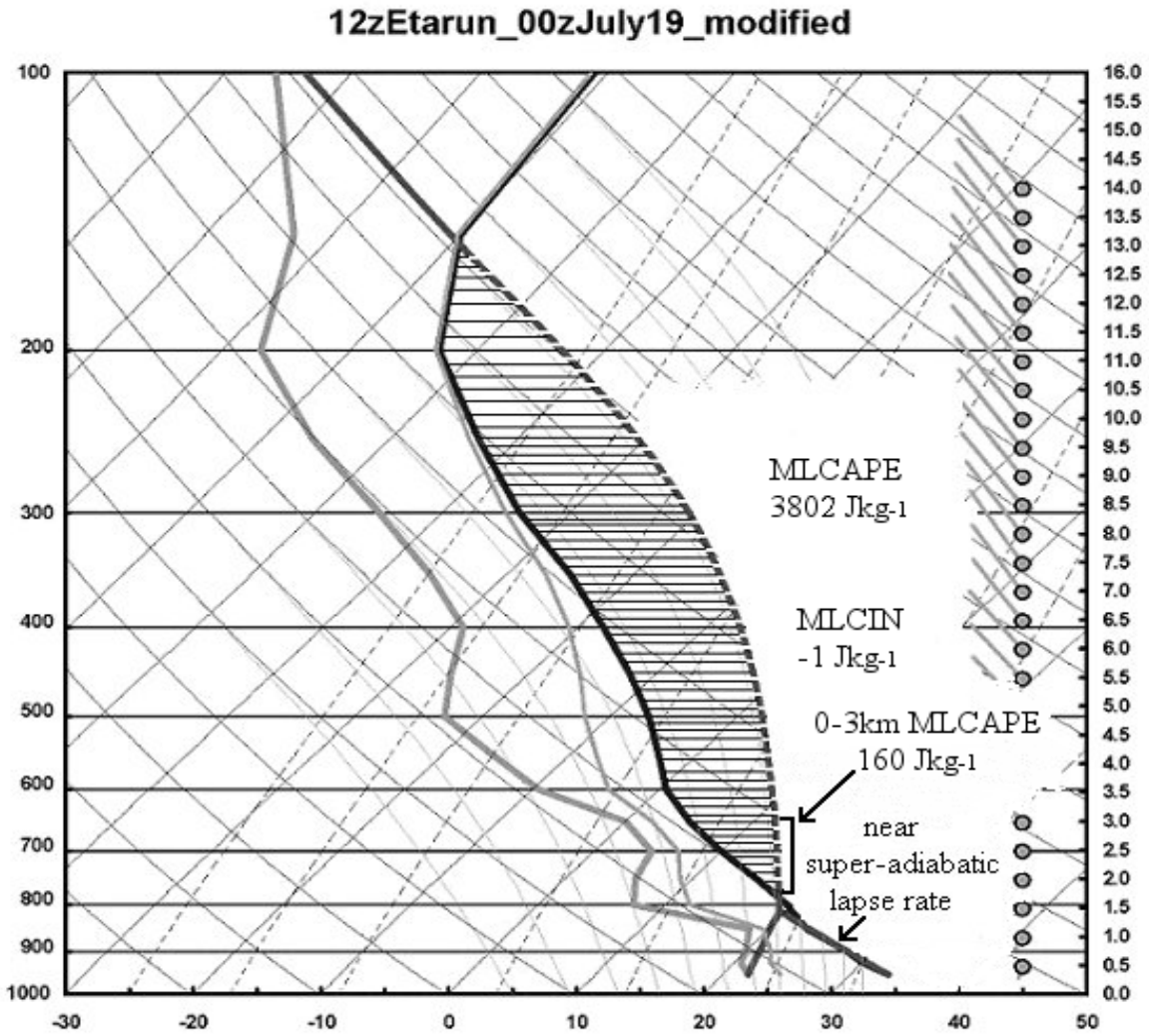


Fig. 14. Same profile as in Fig. 14, except modified to reflect enhanced moisture in the lowest 1000 m based on observed surface dewpoints (3.5 °C greater than forecast in Fig. 13).

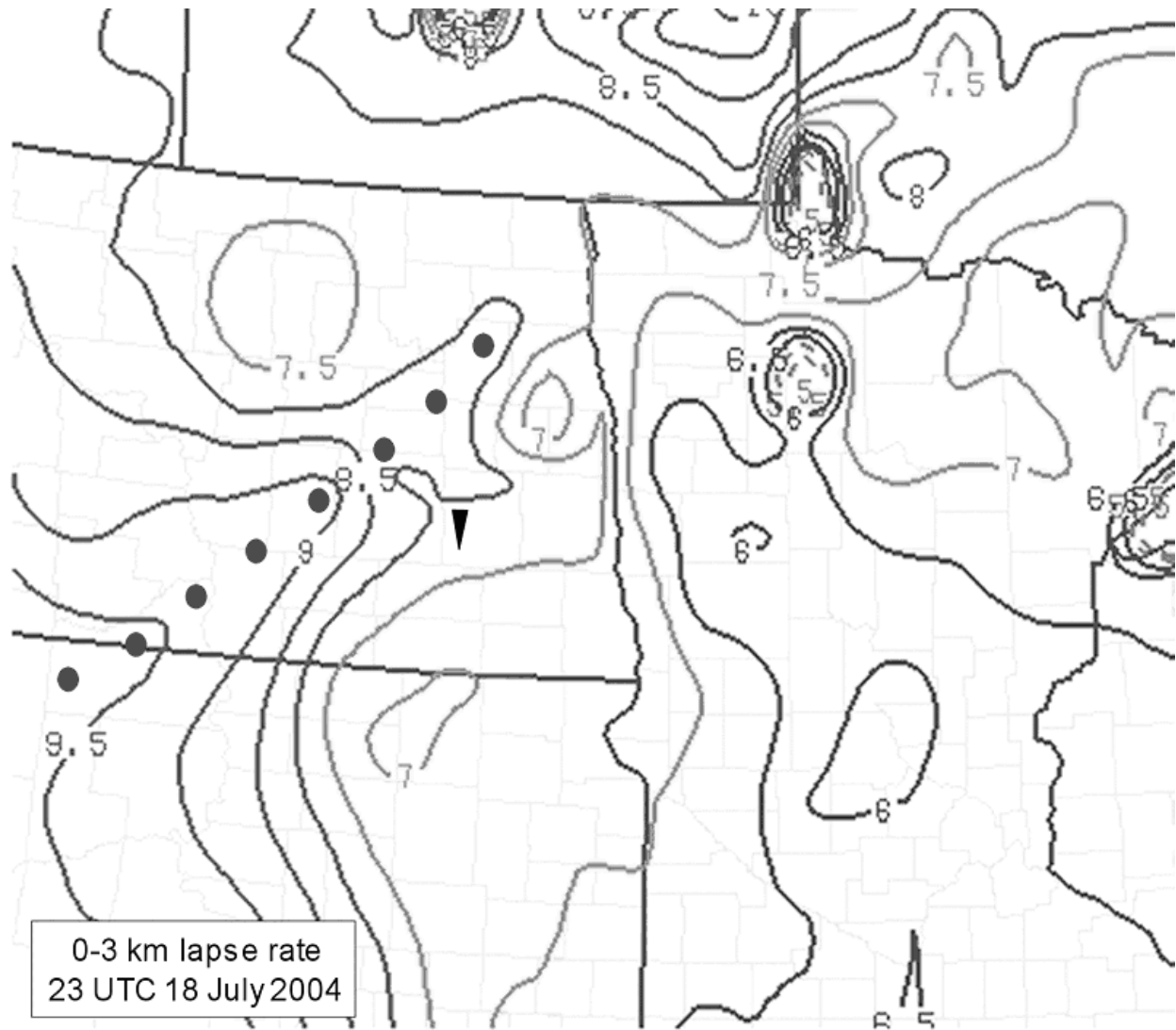
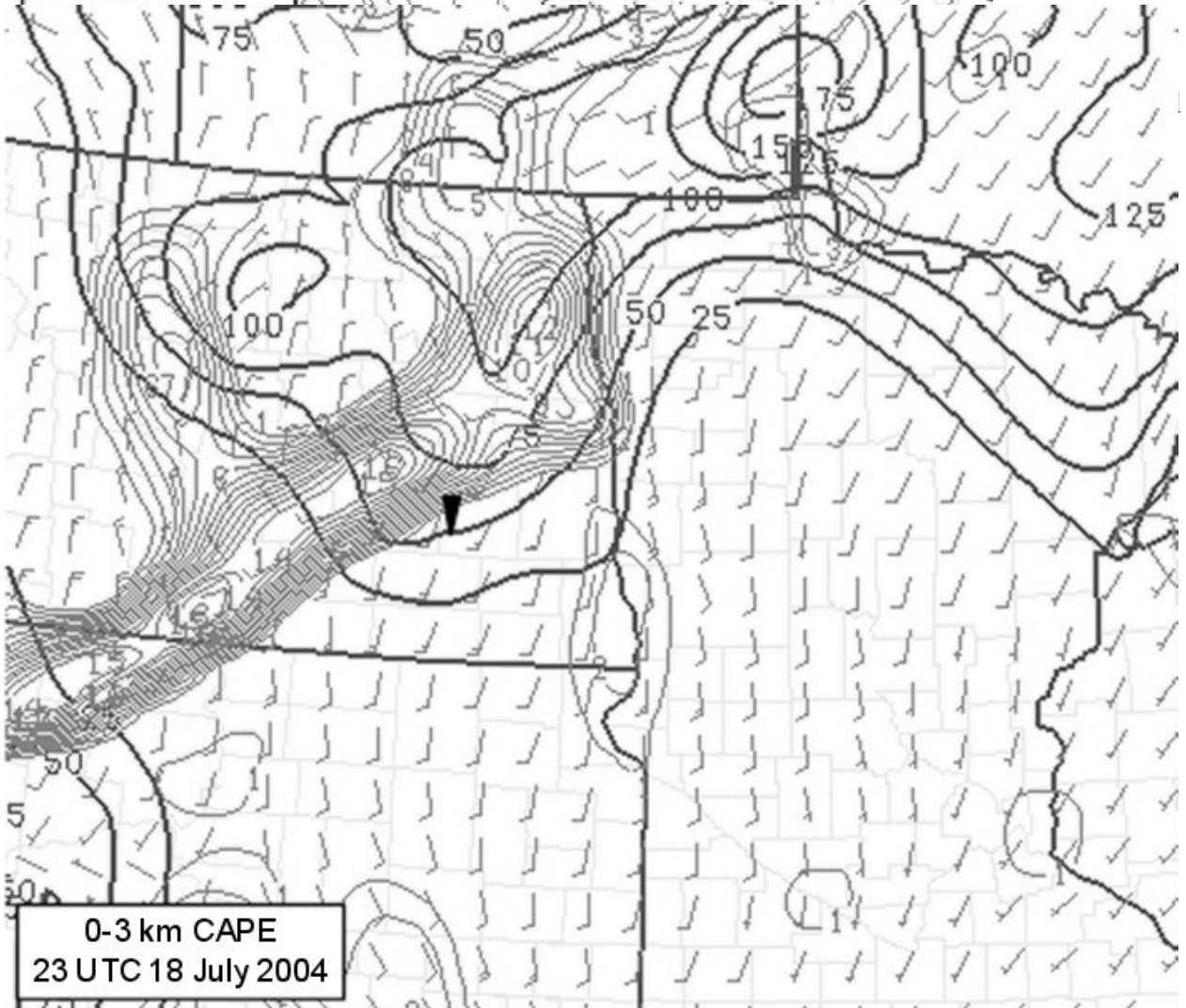
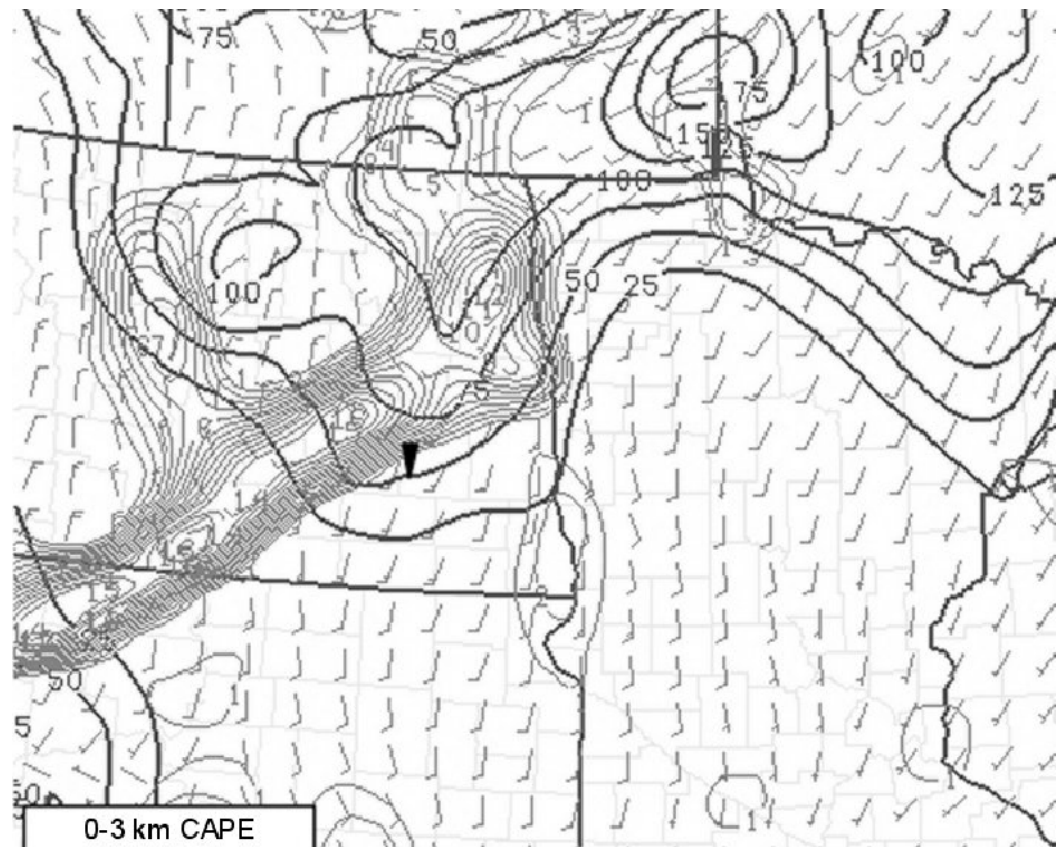


Fig. 15. SPC mesoanalysis of 0-3-km lapse rate ( $^{\circ}\text{C km}^{-1}$  at  $0.5^{\circ}\text{C}$  spacing) at 2300 UTC 18 July 2004. Axis of steepest low-level lapse rates indicated by dots. Location of the F4 tornado shown as in Fig. 2.





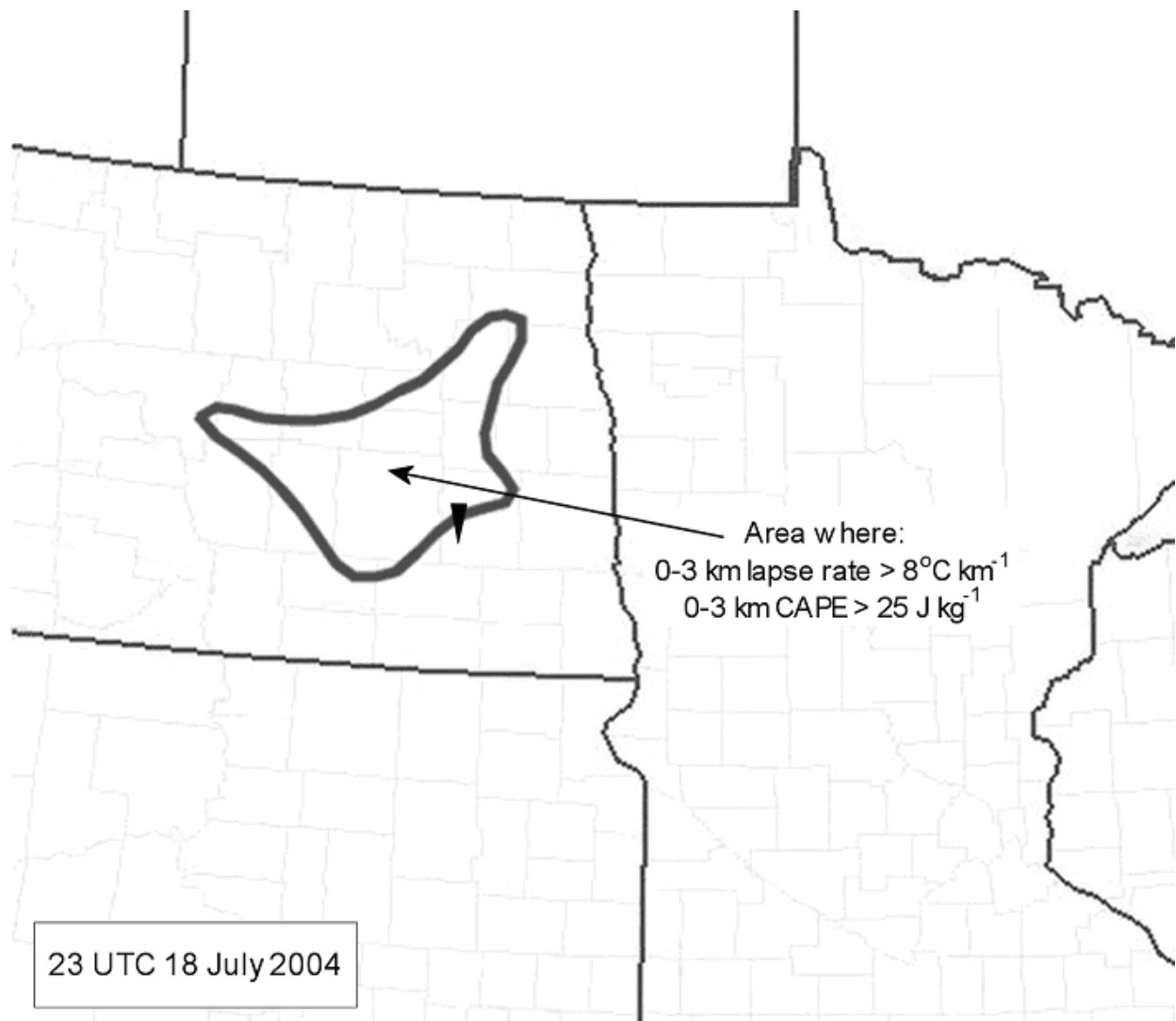


Fig. 17. As in Fig. 15, except area where 0-3-km lapse rates  $\geq 8^{\circ}\text{C km}^{-1}$  overlap 0-3-km CAPE  $\geq 25 \text{ J kg}^{-1}$  from Fig. 17.

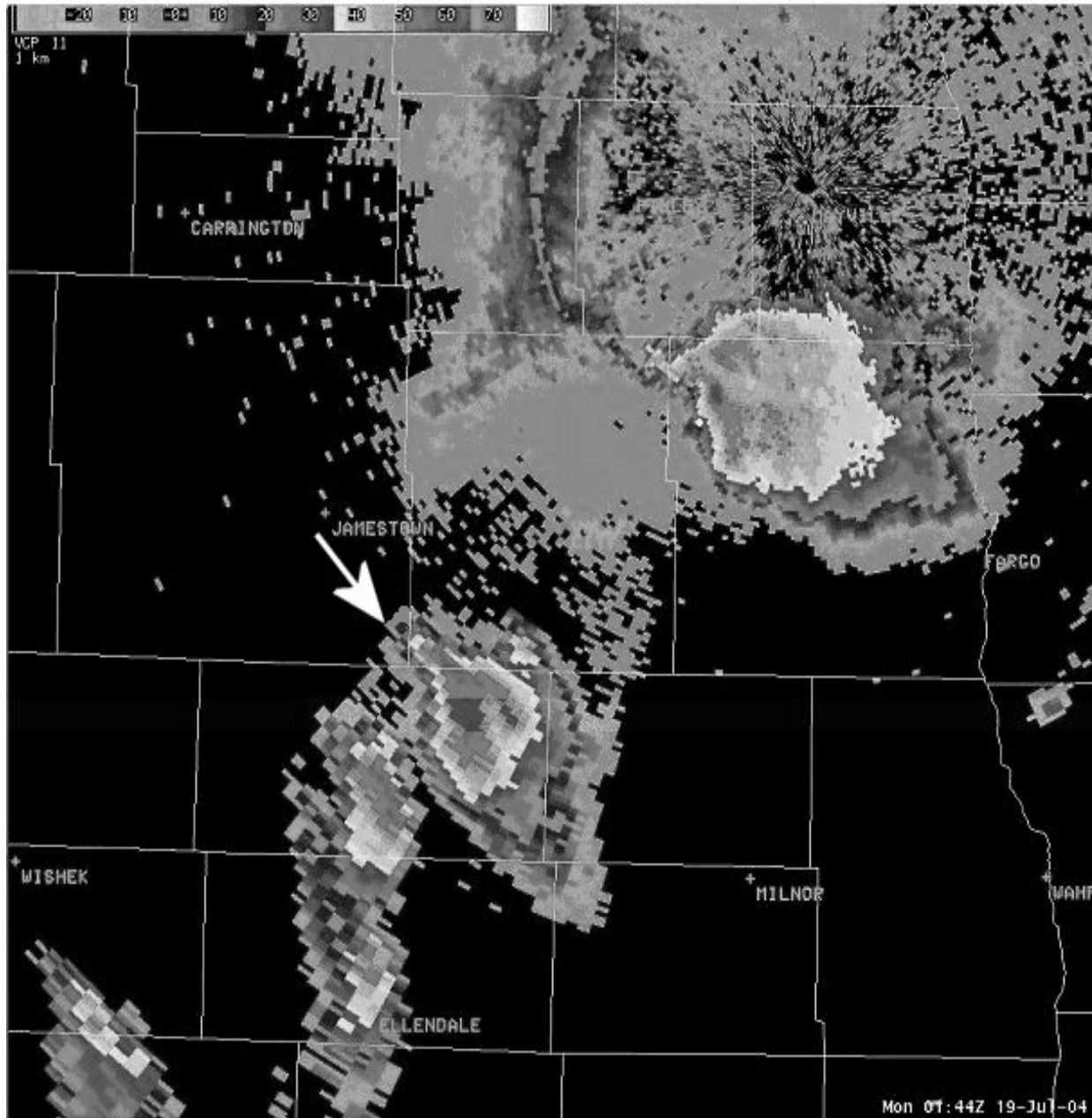


Fig. 18. Mayville, ND WSR-88D (KMVX) base reflectivity at 0144 UTC 19 July 2004. The supercell producing the F4 tornado at the time of this image is indicated by the white arrow.